Development 140, 2310-2320 (2013) doi:10.1242/dev.095653

Cortical excitatory neurons become protected from cell division during neurogenesis in an Rb family-dependent manner

Mio Oshikawa[1], Kei Okada[1], Kazunori Nakajima[2] and Itsuki Ajioka[1,3,*]

SUMMARY

Cell cycle dysregulation leads to abnormal proliferation and cell death in a context-specific manner. Cell cycle progression driven via the Rb pathway forces neurons to undergo S-phase, resulting in cell death associated with the progression of neuronal degeneration. Nevertheless, some *Rb*- and Rb family (*Rb*, *p107* and *p130*)-deficient differentiating neurons can proliferate and form tumors. Here, we found in mouse that differentiating cerebral cortical excitatory neurons underwent S-phase progression but not cell division after acute Rb family inactivation in differentiating neurons. However, the differentiating neurons underwent cell division and proliferated when Rb family members were inactivated in cortical progenitors. Differentiating neurons generated from *Rb*$^{-/-}$*; p107*$^{-/-}$*; p130*$^{-/-}$ (*Rb-TKO*) progenitors, but not acutely inactivated *Rb-TKO* differentiating neurons, activated the DNA double-strand break (DSB) repair pathway without increasing trimethylation at lysine 20 of histone H4 (H4K20), which has a role in protection against DNA damage. The activation of the DSB repair pathway was essential for the cell division of *Rb-TKO* differentiating neurons. These results suggest that newly born cortical neurons from progenitors become epigenetically protected from DNA damage and cell division in an *Rb* family-dependent manner.

KEY WORDS: Cell cycle, Cerebral cortical neurons, Proliferation, Differentiation, DNA damage, Retinoblastoma protein, Mouse

INTRODUCTION

During development, cell cycle exit is tightly coordinated with the initiation of differentiation. Cerebral cortical excitatory neurons are generated from apical progenitors (radial glia cells), basal progenitors (intermediate progenitor cells), and outer radial glia-like progenitors, with coupling to the cell cycle exit of these progenitors (Dehay and Kennedy, 2007; Guillemot et al., 2006; Kriegstein and Alvarez-Buylla, 2009; Tabata et al., 2012). Once the daughter cells initiate neuronal differentiation, they become postmitotic cells and are believed to be protected from cell division (Herrup and Yang, 2007).

Since the discovery of retinoblastoma susceptibility gene 1 (*RB1*) from patients of retinoblastoma (Friend et al., 1986), the Rb pathway has been recognized as the key to regulate cell proliferation, differentiation, and death. These Rb-dependent functions are regulated in a context-specific manner (Burkhart and Sage, 2008; Chau and Wang, 2003; Classon and Harlow, 2002; Weinberg, 1995). For neurons in the central nervous system (CNS), the Rb pathway is believed to prevent cell cycle re-entry, resulting in cell death associated with the progression of neuronal degeneration (Becker and Bonni, 2004; Copani et al., 2001; Heintz, 1993; Herrup and Yang, 2007). This idea was initially supported by the discovery that simian virus 40 (*SV40*) large tumor antigen (*T antigen*) transgenic Purkinje cells in the cerebellum and photoreceptor cells in the retina undergo cell death accompanied by S-phase progression (al-Ubaidi et al., 1992; Feddersen et al., 1995; Feddersen et al., 1992). Moreover, pioneer studies of *Rb*-deficient mice revealed that *Rb*$^{-/-}$ differentiating neurons in the CNS undergo massive cell death accompanied by ectopic S-phase re-entry (Clarke et al., 1992; Jacks et al., 1992; Lee et al., 1992; Lee et al., 1994). However, the cell death of *Rb*-deficient CNS differentiating neurons is caused by the extra-embryonic lineage function of *Rb* (de Bruin et al., 2003). Differentiating cortical neurons survive and proliferate when *Rb* is conditionally deleted before the start of cortical development (Ferguson et al., 2002; MacPherson et al., 2003). In adults, the acute inactivation of *Rb* in mature cortical neurons results in neuronal loss, demonstrating that *Rb* is essential for the survival of mature cortical neurons (Andrusiak et al., 2012). Although these studies clearly demonstrated that *Rb*-deficient differentiating cortical neurons, but not adult mature cortical neurons, escape cell death after S-phase re-entry, acute *Rb* inactivation in cortical differentiating neurons is inevitable for elucidating whether differentiating cortical neurons retain their proliferative potency after neurogenesis or whether the *Rb*-deficient primordium of the cerebral cortex generates proliferative differentiating neurons because of the context-specific roles of *Rb*.

Beyond the context specificities of Rb functions, the complicated compensations and redundancies in *Rb* and its related family members (*p107* and *p130*; *Rbl1* and *Rbl2* – Mouse Genome Informatics) are likely to mask the functions of the Rb family. For example, *Rb*$^{-/-}$ retinal cells in mice do not develop retinoblastoma because of the compensation of *p107* (Chen et al., 2004; MacPherson et al., 2004; Robanus-Maandag et al., 1998; Zhang et al., 2004). p107 is expressed in retinal progenitor cells during the early stages of retinal development, whereas Rb is expressed during the late stages (Donovan et al., 2006). When *Rb* is deleted, p107 is ectopically upregulated during the late stages, compensating for Rb function in the regulation of the progenitor cell cycle. *p130* is also involved in protection against retinal cell proliferation. Rb and p130 are expressed in retinal horizontal interneurons and protect them

[1]Center for Brain Integration Research, Tokyo Medical and Dental University, Tokyo 113-8510, Japan. [2]Department of Anatomy, Keio University School of Medicine, Tokyo 160-8582, Japan. [3]Center for Integrated Medical Research, Keio University School of Medicine, Tokyo 160-8582, Japan.

*Author for correspondence (iajioka@ams.kuramae.ne.jp)

Accepted 3 April 2013

from cell cycle re-entry (Ajioka et al., 2007). p107 is ectopically upregulated in the absence of both Rb and p130; however, *p107* is haploinsufficient for the cell proliferation of differentiated horizontal interneurons. $Rb^{-/-}$; $p107^{+/-}$; $p130^{-/-}$ horizontal interneurons proliferate and develop into metastatic retinoblastoma. Therefore, careful genetic study is required to elucidate the functions of Rb family members in the neurogenesis and differentiation of cortical neurons.

In this study, to elucidate the Rb family roles in cortical excitatory neurons and their progenitors, all the Rb family members were inactivated in differentiating neurons and progenitors using a neuron-specific pMAP2 promoter and a ubiquitous pCAG promoter, respectively, together with the *in utero* electroporation method. We found that pMAP2-induced *Rb-TKO* (pMAP2-*Rb-TKO*) differentiating neurons undergo S-phase, but not cell division. However, pCAG-induced *Rb-TKO* (pCAG-*Rb-TKO*) cells initiated differentiation without undergoing cell cycle exit and the trimethylation of lysine 20 of histone H4 (H4K20), but proliferated. pCAG-*Rb-TKO* differentiating neurons were not trimethylated at H4K20 and activated the double-strand break (DSB) repair pathway, leading to G2/M-phase progression. Thus, the activation of the DSB repair pathway is essential for the uncoupled proliferation and differentiation of *Rb-TKO* cortical excitatory neurons.

MATERIALS AND METHODS

Mice

$Rb^{Lox/Lox}$; $p107^{-/-}$; $p130^{Lox/Lox}$ mice were obtained from Michael Dyer (St Jude Children's Research Hospital, USA). $Rb^{Lox/Lox}$ mice were originally produced by Anton Berns (Netherlands Cancer Institute, The Netherlands). The *p107* knockout mice were originally produced by Tyler Jacks (Massachusetts Institute of Technology, USA). $p130^{Lox/Lox}$ mice were originally produced by Julien Sage (Stanford University, USA). *Z/EG* mice were originally produced by Corrinne Lobe (Miami Mice Research Corp., Canada). Pregnant ICR mice were purchased from Sankyo Lab Service Corporation (Tokyo, Japan). The animal experiment procedures were approved by the Animal Experiment Committee of Tokyo Medical and Dental University.

Plasmids

pCAG-Cre and pCAG-CreERT2 plasmid was obtained from Connie Cepko (Harvard Medical School, USA) and the human *MAP2* gene promoter was obtained from Vijayasaradhi Setaluri (University of Wisconsin, USA). To generate Cre-expressing plasmid under a *MAP2* promoter, pDsRed-Express2-1 plasmid (Clontech, CA, USA) was digested using *Sma*I and *Ale*I and DsRed cDNA was then removed. Next, we generated pMCS-Cre by inserting Cre cDNA into the *Eco*RI site. To generate pMAP2-Cre, MAP2 promoter region was cut out from a phMAP2-1 plasmid using *Hin*dIII and was inserted into pMCS-Cre. To generate pMAP2-CreERT2, CreERT2 cDNA was cut out from pCAG-CreERT2 using *Not*I and *Pvu*I and swapped for the cDNA of pMAP2-Cre.

Dissection of the cerebral cortex, the VZ/SVZ, the IZ and the CP

The cerebral hemispheres were dissected out from E14 and E16 mice, and the anterior one-third and the posterior one-third of the specimens were removed. After removing the meninges, the ventricular/subventricular zone (VZ/SVZ), the intermediate zone (IZ), and the cortical plate (CP) of the E16 specimens were manually dissected from the lateral cortices under a stereoscopic microscope (Ajioka and Nakajima, 2005).

Electroporation

For the *in utero* electroporation, pCAG-Cre and pMAP2-Cre were injected into the lateral ventricle of E14 mouse embryos. The cells attached to the ventricular surface were transfected using 35 V square pulse electroporation (NEPA21; Nepagene, Chiba, Japan), as described previously (Tabata and Nakajima, 2001). At P2 and P10, the transfected mice were perfusion fixed with 4% paraformaldehyde and the brains were cryosectioned.

For the *ex vivo* electroporation, we modified a protocol used for retinal explants (Donovan and Dyer, 2007). Briefly, the dissected cerebral cortex from E14 mice was transferred to a Petri dish electrode chamber filled with plasmid solution and was transfected using 25 V square pulse electroporation (NEPA21). The transfected cerebral cortex was transferred to a polycarbonate membrane (Whatman, NJ, USA) on explant medium [Dulbecco's modified Eagle medium: Nutrient Mixture F-12 medium (Sigma, MO, USA) supplemented with 10% fetal bovine serum (FBS; Invitrogen, NY, USA), 10 mM HEPES (Invitrogen), penicillin/streptomycin/glutamine (Invitrogen), and insulin (Sigma)] and was cultured for 2 to 7 days.

Immunostaining

For immunohistochemistry (IHC), the cryosections were post-fixed in 4% paraformaldehyde for 16 hours at 4°C, in general, and in 2% paraformaldehyde for 1 hour at 4°C for Rb, p107 and p130 staining, preincubated with 2% normal goat or donkey serum for 1 hour at room temperature, and incubated with 1/1000 chicken anti-GFP (ab13970, Abcam, MA, USA), 1/300 rabbit anti-Ki-67 (ab15580, Abcam), 1/1000 mouse anti-neuron specific beta III tubulin (Tuj1) (ab78078, Abcam), 1/5000 rabbit anti-Pax6 (PRB-278P, Covance, CA), 1/500 rabbit anti-Tbr2 (ab23345, Abcam), 1/1000 rabbit anti-DCX (ab18723, Abcam), 1/100 rabbit anti-SATB2 (ab51502, Abcam), 1/500 anti-Ctip2 (ab18465, Abcam), 1/500 anti-Tbr1 (ab31940, Abcam), 1/200 rat anti-phospho S28 histone H3 (ab10543, Abcam), 1/1000 rabbit anti-active caspase-3 (557035, BD, NJ, USA), 1/1000 anti-CD31 (ab28364, Abcam), 1/1000 anti-Olig2 (BAF2418, R&D Systems, MN, USA), 1/500 rabbit anti-Rb (ab39538, Abcam), 1/100 rabbit anti-p107 (sc-318, Santa Cruz, CA, USA), 1/100 rabbit anti-p130 (sc-317, Santa Cruz), 1/1000 rabbit anti-phospho S139 H2AX (ab2893, Abcam), 1/300 rabbit anti-H4K20Me3 (ab9053, Abcam), 1/3000 rabbit anti-H4K20Me1 (ab9051, Abcam), or 1/1000 rabbit anti-H3K9Me3 (07-523, Upstate, NY, USA) overnight at 4°C. For Pax6 and H4K20Me1 staining, the cryosections were pretreated at 90°C for 5 minutes before the primary antibody reaction. The primary antibodies were visualized using Alexa Fluor 488 goat anti-chicken IgG (Invitrogen), Alexa Fluor 546 goat anti-mouse, anti-rabbit, and anti-rat IgG (Invitrogen), and Alexa Fluor 647 goat anti-mouse and anti-rabbit IgG (Invitrogen). For Olig2 and Tbr2 staining, the primary antibodies were reacted with biotinylated anti-rabbit IgG (Vector, CA, USA) followed by VECTASTAIN ABC reagent (Vector) and then visualized with Cy3-thyramide (PerkinElmer, MA, USA). The nuclei were counterstained with 2 μg/ml of 4′,6-diamidino-2-phenylindole (DAPI, Sigma) and 1/1000 TO-PRO3 (Invitrogen). Fluorescence images were obtained using a confocal microscope (LSM510; Zeiss, Oberkochen, Germany). Structured illumination microscope (SIM) images were obtained using a super-resolution microscope (ELYRA; Zeiss).

For immunocytochemistry (ICC), the explant cells were treated with 100 μg/ml of trypsin in Ca^{2+}- and Mg^{2+}-free phosphate buffered saline (PBS) for 5 minutes at 37°C. After gentle tapping, the cells were incubated for an additional 5 minutes at 37°C and were dissociated by tapping. Then, the cells were incubated with 100 μg/ml of trypsin inhibitor (Sigma) and 20 μg/ml of DNase (Sigma) in PBS with Ca^{2+} and Mg^{2+} for 5 minutes at 37°C. After adding five volumes of explant medium, the cells were plated on poly-L-lysine-coated slide glass and incubated for 1 hour at 37°C. The attached cells were fixed with 4% PFA for 1 hour at 4°C, preincubated with 2% normal goat or donkey serum for 1 hour at room temperature, and incubated with the primary antibodies described above.

For EdU staining, 50 μg/g body weight of EdU (Invitrogen) was intraperitoneally injected for *in vivo* labeling, and 3 μg/ml of EdU was added 1 hour or 16 hours before cell dissociation for *in vitro* labeling. EdU-incorporated cells were visualized using Alexa Fluor 594 after the primary antibody reaction.

The ratio of immunopositive cells was quantified with unbiased optical fractionator approach (Stereo Investigator, Micro Bright Field, VT, USA). Fluorescence images were obtained using a fluorescence microscope (BX51; Olympus, Tokyo, Japan).

Western blotting

The dissected VZ, IZ, and CP and cerebral cortex tissues were dissolved in lysis buffer [20 mM Tris (pH 7.4), 150 mM NaCl, 1 mM ethylene-diamine-

tetra-acetic acid (EDTA), 1% NP-40, and protease inhibitor (complete, EDTA-free; Roche, Upper Bavaria, Germany)], and the samples were centrifuged at 15,000 ***g*** for 5 minutes. The supernatants were dissolved in sodium dodecyl sulfate (SDS) loading buffer and subjected to SDS-polyacrylamide gel electrophoresis (SDS-PAGE) on 7.5% and 12% polyacrylamide gels. The proteins were then electroblotted on to polyvinylidene fluoride membranes using an iBlot Gel Transfer Device (Invitrogen). The membranes were incubated with 1/5000 mouse anti-RB (554136, BD), 1/5000 rabbit anti-p107, 1/5000 rabbit anti-p130, 1/1000 mouse anti-MAP2 (MAB3418, Millipore, MA, USA), 1/1000 rabbit anti-EphA3 (sc-919, Santa Cruz), 1/5000 mouse anti-PCNA (ab29, Abcam), and 1/10,000 mouse anti-beta-actin (ab6276, Abcam) for 16 hours at 4°C after blocking with 5% skim milk for 1 hour at room temperature, and then with 1/5000 peroxidase-labeled goat anti-mouse and anti-rabbit IgG (DAKO, Glostrup, Denmark) for 2 hours. The bands were detected using SuperSignal West Femto Maximum Sensitivity Substrate (Thermo Fisher, MA, USA) and were visualized using Chemi Doc XRS-J (Bio-Rad, CA, USA).

Gene expression array analysis

The GFP-positive cells were dissociated from explant cultured for 4 days, labeled with 100 ng/ml DAPI to remove dead cells, and then sorted using a FACS Vantage SE (BD). Ten nanograms of the total RNA was purified from 3×10^4 cells using an RNeasy Micro Kit (Qiagen, Venlo, Netherlands) (n=3). The concentration and integrity of the total RNA was measured using an RNA6000 Pico Kit (Agilent, CA, USA) and a 2100 Bioanalyzer (Agilent). The total RNA was amplified following a One-Color Microarray-Based Gene Expression Analysis (Low Input Quick Amp Labeling), version 6.0. The amplified cRNA (1.5 μg) was hybridized on an Agilent Whole Mouse Genome Array (4×44K), version 2.0, for 17 hours. The chips were scanned on an Agilent DNA Microarray Scanner using Feature Extraction software, version 10.7.1.1 (Agilent). The cRNA synthesis and hybridization were performed at Chemicals Evaluation and Research Institute (CERI) (Tokyo, Japan). The data were analyzed using GeneSpring software, ver. 11.5. (Agilent). All the array data were deposited in the GEO public database (accession no. GSE37577).

Real-time RT-PCR

First strand cDNA was synthesized from 1 μg total RNA from dissected tissues and 10 ng of total RNA from FACS-sorted cells with 100 pmol of T7-$(dT)_{24}$ primer and 200 units of Superscript III (Invitrogen) at 42°C for 1 hour. The real-time RT-PCR was performed using SsoFast Probes Supermix (Bio-Rad) and the CFX96 system (Bio-Rad). The primer sequences are described in supplementary material Table S1. The gene expression levels were normalized to the *Gapdh* and *Gpi1* expression levels.

RESULTS

Expression profiles of Rb family members during cerebral cortical development

To begin to address the role of Rb family members in the neurogenesis and differentiation of cortical excitatory neurons, we examined the expression profiles of Rb family members in the developing cerebral cortex. We performed a real-time RT-PCR and a western blotting analysis using manually dissected VZ and SVZ where cortical excitatory neurons are generated, the IZ where differentiating neurons migrate, and the CP where differentiating

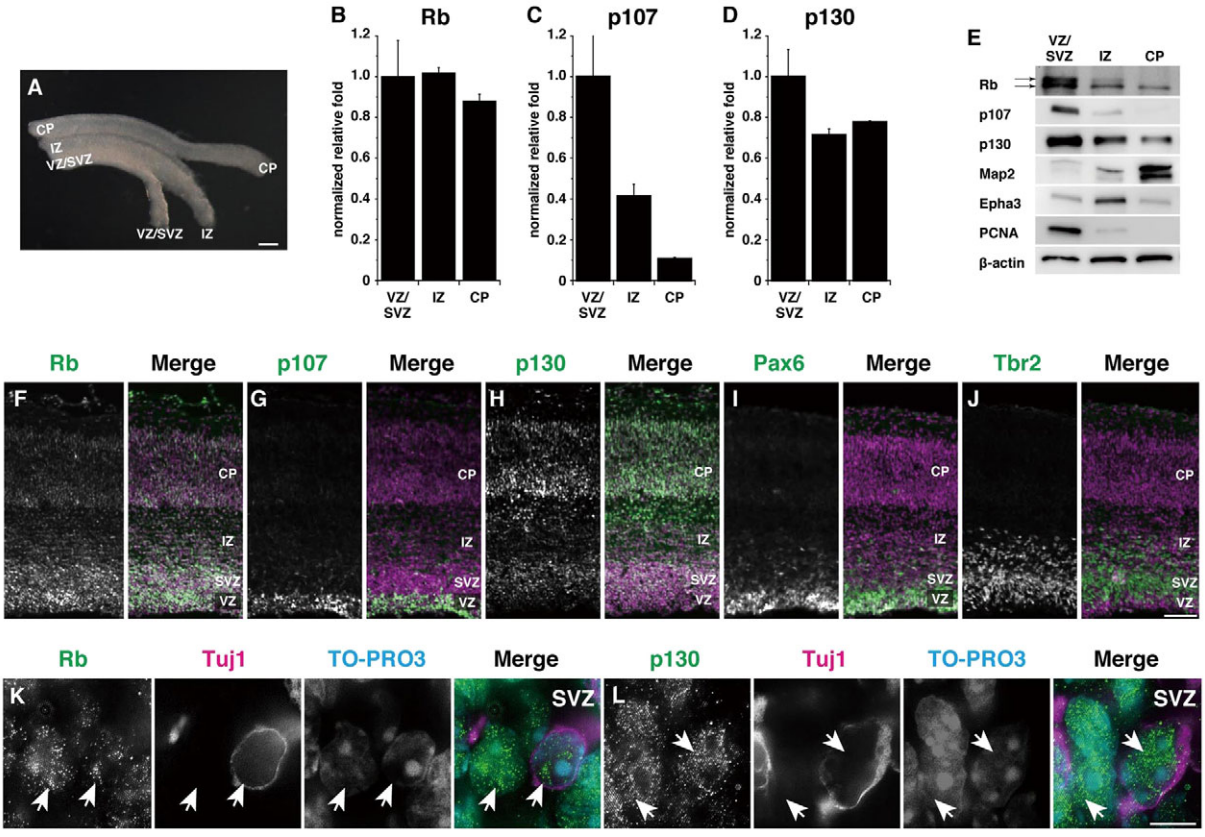

Fig. 1. Rb family expression during mouse cortical development. (**A**) The E16 VZ/SVZ, IZ and CP tissues were manually dissected under a stereoscopic microscope. (**B-D**) Real-time RT-PCR for Rb (B), p107 (C) and p130 (D) of the dissected VZ/SVZ, IZ and CP tissues. (**E**) Immunoblot for Rb, p107, p130, Map2, Epha3, PCNA and β-actin of the dissected tissues. (**F-J**) Immunofluorescent staining for Rb (F), p107 (G), p130 (H), Pax6 (I) and Tbr2 (J) appears white in the single images and green in the merged images in E16 cerebral cortex. The nuclei (magenta) were counterstained and the images were merged. (**K**,**L**) SIM images of Rb (K) and p130 (L) with Tuj1-antigen. Arrows: Rb- (K) and p130- (L) positive areas. Scale bars: 100 μm in A,J; 5 μm in L.

neurons align, according to a previously reported method (Ajioka and Nakajima, 2005) (Fig. 1A-E). As previously reported using an *in situ* hybridization analysis (Jiang et al., 1997), all the Rb family member mRNAs and proteins were expressed in the VZ/SVZ (Fig. 1B-E). Both Rb and p130, but not p107, were detected in the CP (Fig. 1E). To determine more specific regions where Rb family member proteins are enriched, we performed immunohistostaining. In the VZ where the apical progenitor marker Pax6 was enriched (Fig. 1I), both Rb and p107 proteins were detected (Fig. 1F,G). By contrast, in the SVZ where the basal progenitor marker Tbr2 (Eomes – Mouse Genome Informatics) was enriched (Fig. 1J), both Rb and p130 proteins were detected (Fig. 1F,H). As cortical excitatory neurons start to differentiate and express neuronal markers in the SVZ, we performed double staining for Rb and p130 using the neuronal marker Tuj1 (Tubb3 – Mouse Genome Informatics) antigen to determine whether Rb and p130 protein are enriched in both progenitors and differentiating neurons or in one or the other. A SIM image analysis revealed that both Rb and p130 were detected at the nuclei in both Tuj1-positive and -negative cells (Fig. 1K,L). Together, these results suggested that apical progenitors express both Rb and p107, whereas

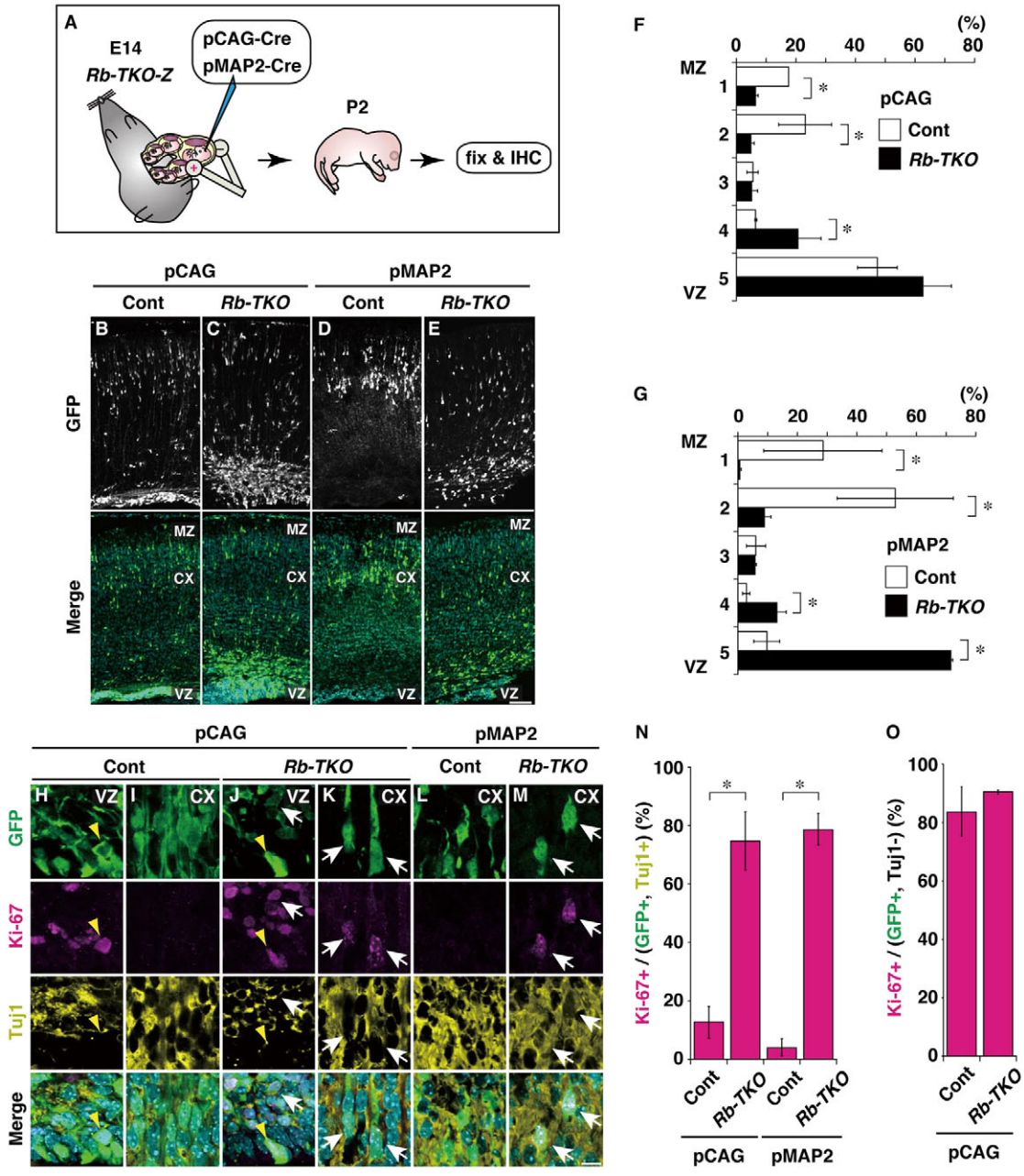

Fig. 2. Migration defect and cell cycle activation of *Rb-TKO* differentiating neurons. (**A**) Experiment scheme. (**B-E**) Immunofluorescent staining for GFP in P2 telencephalon. The nuclei (cyan) were counterstained with DAPI and the images were merged. *Z/EG* mice were used as a control. (**F**,**G**) Distribution of GFP-positive cells labeled using pCAG-Cre (F) and pMAP2-Cre (G) in *Rb-TKO-Z* and a control. The cortical area was equally divided into five areas from the MZ to the VZ. (**H-M**) Immunofluorescent staining for GFP (green), Ki-67 (magenta), Tuj1 (yellow) and DAPI (cyan) at the VZ (H,J) and the cortex (CX) (I,K,L,M) of *Rb-TKO-Z* and a control. Arrows: GFP, Ki-67, and Tuj1 triple-positive cells. Arrowheads: GFP and Ki-67 double-positive and Tuj1-negative cells. (**N**,**O**) Ratio of Ki-67-positive cells to Tuj1 and GFP double-positive cells (N) and Tuj1-negative and GFP-positive cells (O) scored in immunostained tissues. **P*<0.05. Scale bars: 50 μm in E; 10 μm in M.

basal progenitors and differentiating neurons express both Rb and p130. Thus, we examined the roles of Rb family members in cortical excitatory neurons by inactivating all the Rb family members.

Role of the Rb family in the development of cortical excitatory neurons

To elucidate the roles of Rb family members in the neurogenesis and differentiation of cortical excitatory neurons, we transfected a Cre-expressing plasmid into *Z/EG; $Rb^{Lox/Lox}$; $p107^{-/-}$; $p130^{Lox/Lox}$* (*Rb-TKO-Z*) cortical progenitors using *in utero* electroporation on embryonic day (E) 14 (Fig. 2A). To inactivate the Rb family members in the progenitors and differentiating neurons, we used a ubiquitous pCAG promoter and a neuron-specific pMAP2 promoter, respectively. Immunostaining for the *Z/EG* reporter protein GFP revealed that the start of both pCAG-Cre and pMAP2-Cre activation in the VZ/SVZ (supplementary material Fig. S1A-F). Using a 5-ethynyl-2′-deoxyuridine (EdU) labeling experiment, we confirmed that pMAP2-Cre activated the *Z/EG*-reporter gene preferentially in non-dividing cells (supplementary material Fig. S1A-E,G). Dissociated cell scoring also confirmed that pCAG-Cre, but not pMAP2-Cre, labeled Dcx-negative progenitor cells (supplementary material Fig. S1H,I). Although many GFP- and EdU-positive cells were detected in the CP (supplementary material Fig. S1B,D), most of the EdU-positive cells were positive for the glial progenitor marker Olig2 and endothelial cell marker Cd31 (Pecam1 – Mouse Genome Informatics) (supplementary material Fig. S1J-L). At 24 hours after the electroporation of both pCAG-Cre and pMAP2-Cre, the reporter GFP protein was detected near the VZ/SVZ (supplementary material Fig. S1M,N). These results suggest that the start of pMAP2-Cre activation occurred just after neurogenesis. When the transfected cells were analyzed on postnatal day (P) 2, *Rb-TKO* cells labeled with both pCAG and pMAP2 were located near the VZ (Fig. 2C,E-G), whereas the control cells had migrated in the cortex (Fig. 2B,D,F,G). These data suggested that acute Rb family inactivation impaired migration in the developing cerebral cortex.

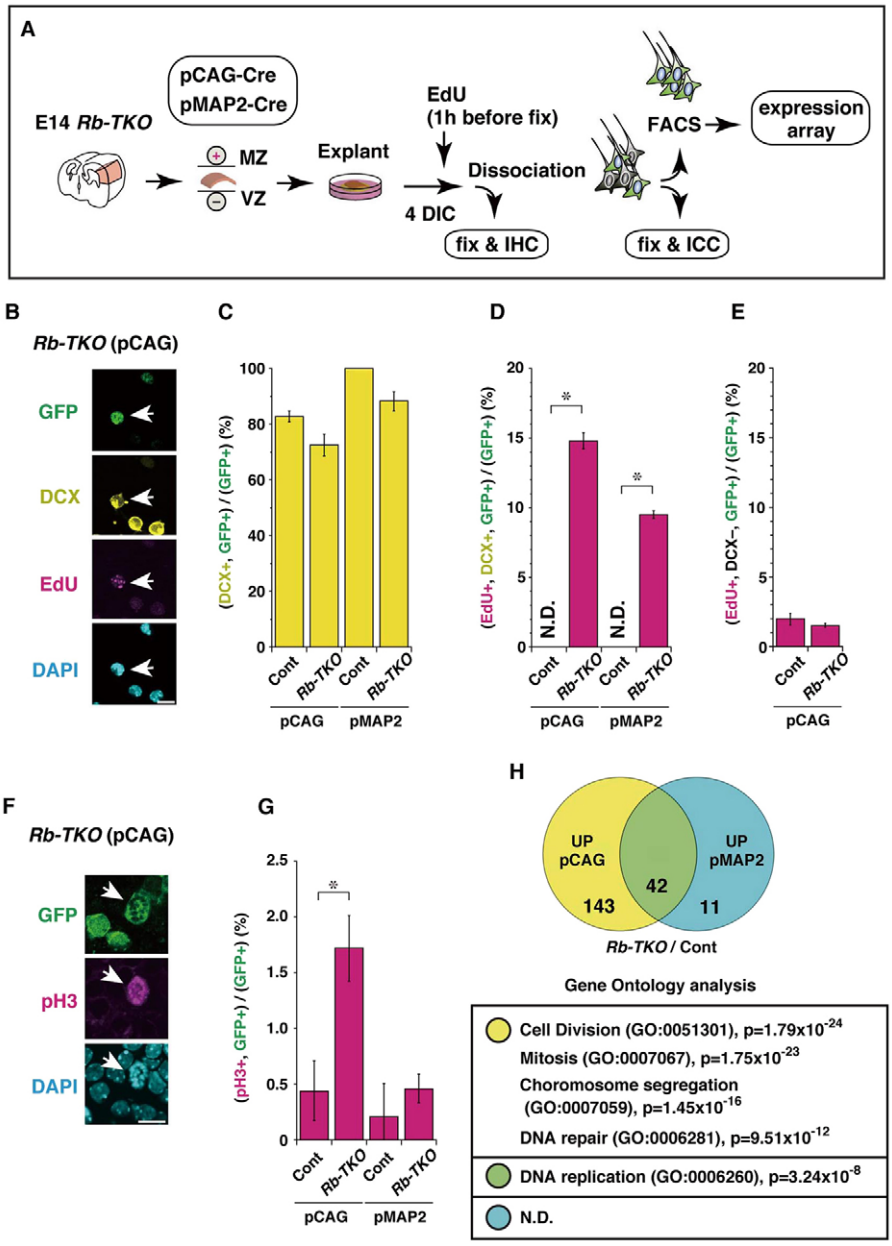

Fig. 3. Cell division of differentiating neurons by Rb family inactivation in progenitors, but not in neurons. (**A**) Experiment scheme. (**B**,**F**) Immunofluorescent images for GFP (green), EdU (B) or pH3 (F) (magenta), Dcx (B) (yellow) and DAPI (cyan) in *Rb-TKO-Z* cells. Arrows: immunopositive cells. (**C-E**,**G**) Ratios of Dcx and GFP double-positive cells (C), EdU, Dcx and GFP triple-positive cells (D), EdU and GFP double-positive and Dcx-negative cells (E), and pH3 and GFP double-positive cells (G) to total GFP-positive cells. (**H**) GO analysis with a Venn diagram showing genes upregulated by more than threefold after Rb family inactivation by pCAG-Cre and pMAP2-Cre. **P*<0.05. Scale bars: 10 μm.

To determine whether Rb family members regulate the cell cycle exit of progenitors and the cell cycle re-entry of differentiating neurons, green fluorescent protein (GFP)-positive cells were co-stained with Ki-67 antigen, the expression of which disappears at G0-phase (Gerdes et al., 1984). A cell scoring analysis revealed that most of the pCAG- and pMAP2-*Rb-TKO* cells were co-stained with Ki-67 and Tuj1 (Fig. 2H-N). The ratio of Ki-67-positive and Tuj1-negative cells was not significantly different between the control and *Rb-TKO* cells (Fig. 2O). The Ki-67-positive *Rb-TKO* cells were detected throughout the cortex (supplementary material Fig. S2A,B). To reduce the possibility that the migration defect triggered the cell cycle re-entry of *Rb-TKO* cells, we injected pMAP2-CreERT2 plasmid and inactivated Rb family members using tamoxifen injection at P0 and P1 after the completion of migration. Even after the acute inactivation at postnatal stages, *Rb-TKO* cells expressed the Ki-67 antigen (supplementary material Fig. S2C-E). These results suggest that Rb family members are essential for the cell cycle exit of progenitors and the prevention of the cell cycle re-entry of differentiating neurons. To characterize the neurogenesis and differentiation of the *Rb-TKO* progenitors, the GFP-positive cells were co-stained with various markers. Although some *Rb-TKO* cells expressed undifferentiated cell markers (supplementary material Fig. S2F-K), most of the *Rb-TKO* cells expressed the neuronal marker Dcx (supplementary material Fig. S2L-N). Ectopically located *Rb-TKO* cells expressed the layer II/III and V marker Satb2 near the VZ (supplementary material Fig. S2O,P,S), and these cells co-expressed Ki-67 (Mki67 – Mouse Genome Informatics) (supplementary material Fig. S2T). However, *Rb-TKO* cells did not express the early-born neuron markers Tbr1 and Ctip2 (Bcl11b – Mouse Genome Informatics) (supplementary material Fig. S2Q-S). These results suggest that the daughter cells of *Rb-TKO* progenitors ectopically initiate the proper differentiation program without exiting the cell cycle.

Neuronal expansion derived from *Rb-TKO* cortical progenitors, but not acutely inactivated differentiating neurons

To examine whether *Rb-TKO* differentiating neurons advance their cell cycle, we performed cell scoring using EdU and the G2/M-phase marker phosphohistone-H3 (pH3) in addition to a genome-wide gene expression array analysis. We used the *in vitro* electroporation method, modified from a protocol developed for retinal explants, because of the advantage of the high transfection efficiency (Donovan and Dyer, 2007) (Fig. 3A). The cortical cells *in vitro* migrated toward the marginal zone (MZ) and developed dendrites, as observed *in vivo* (supplementary material Fig. S3A-D). Ki-67 antigen became detectable from 48 hours in both pCAG- and pMAP2-*Rb-TKO* cells, suggesting that both pCAG- and pMAP2-*Rb-TKO* cells lose Rb family proteins at almost same time (supplementary material Fig. S3E). To determine whether Dcx-positive pCAG- and pMAP2-*Rb-TKO* cells undergo S-phase, we added EdU at 1 hour before fixation. A dissociated cell scoring analysis revealed that Dcx-positive *Rb-TKO* cells entered S-phase when the Rb family members were inactivated by pCAG-Cre and pMAP2-Cre (Fig. 3B-D). By contrast, the ratio of cells in S-phase did not change in Dcx-negative *Rb-TKO* cells (Fig. 3E). To exclude the possibility that DNA damage-induced

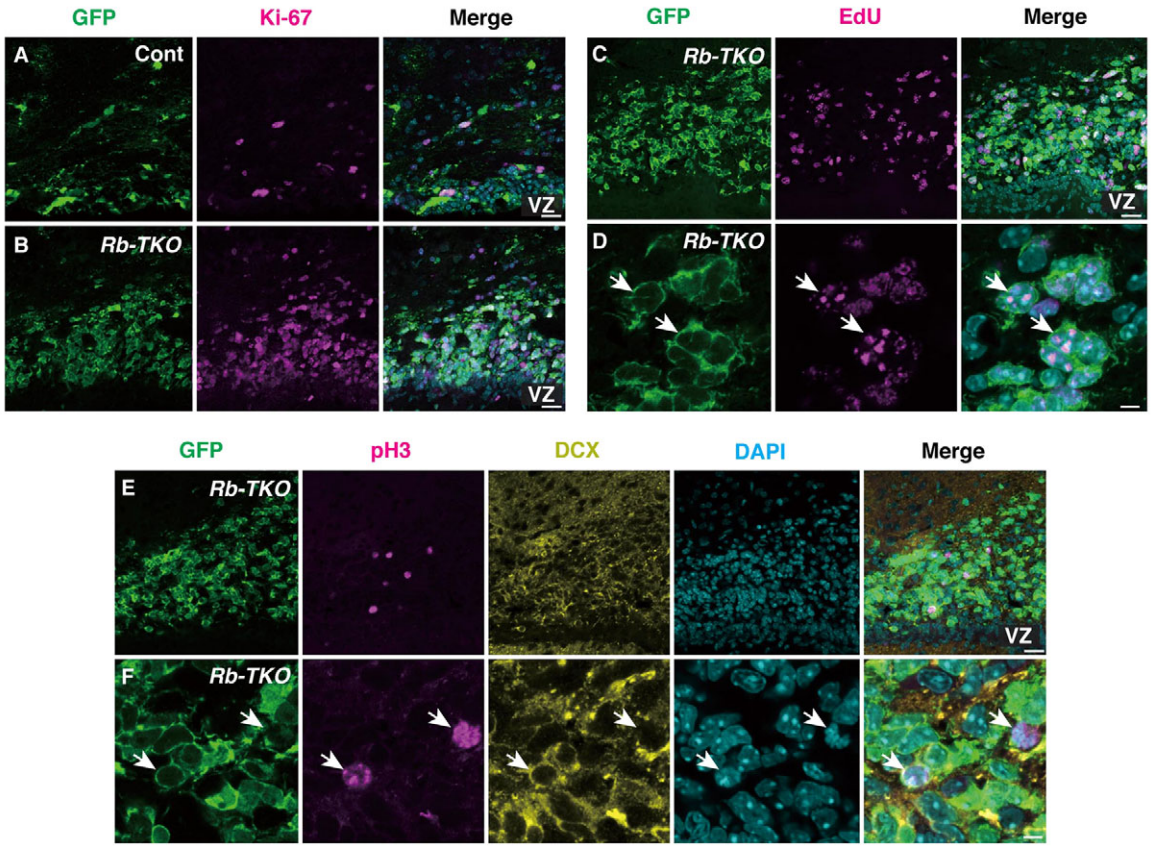

Fig. 4. Expansion of differentiating neurons generated from *Rb-TKO* progenitors. (**A-F**) Immunofluorescent staining for GFP (green), Ki-67 (A,B), EdU (C,D) or pH3 (E,F) (magenta), Dcx (E,F) (yellow) and DAPI (cyan) in pCAG-Cre-transfected P10 cerebral cortex of control (A) and *Rb-TKO-Z* (B-F) near the VZ. Scale bars: 50 μm in A-C,E; 10 μm in D,F.

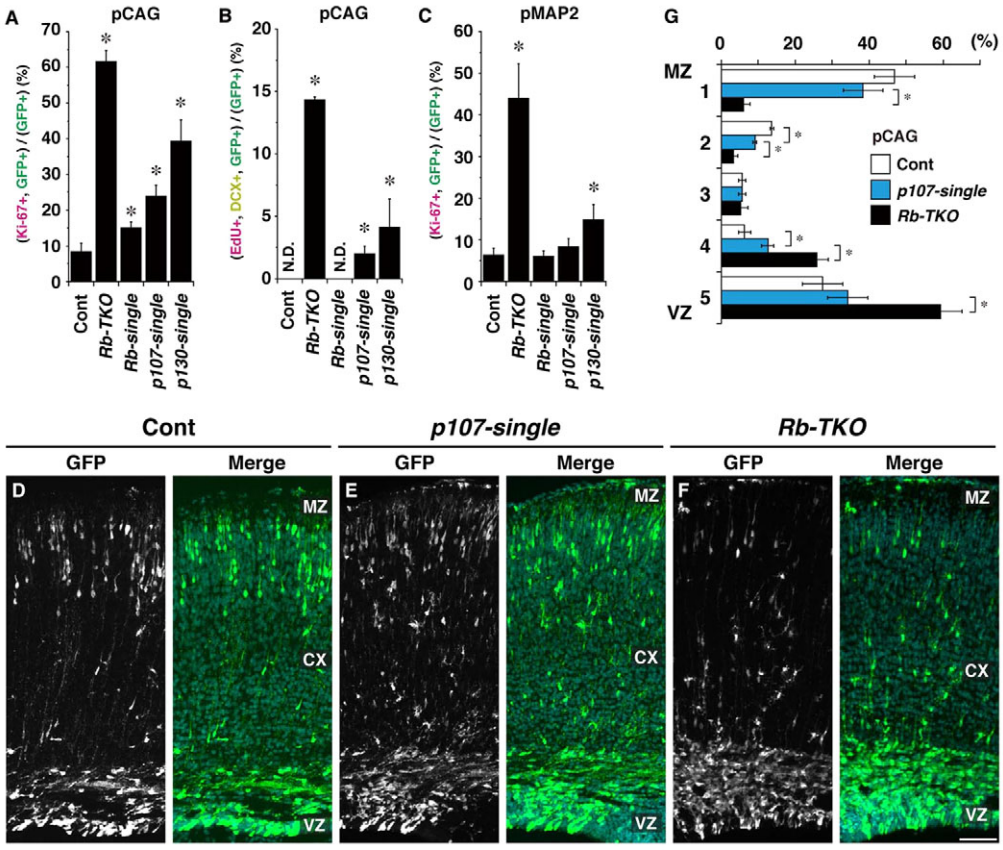

Fig. 5. Compensation of *p107* in the absence of *Rb* and *p130* in differentiating neurons. (**A-C**) Ratios of GFP and Ki-67 double-positive cells (A,C) and GFP, EdU, and Dcx triple-positive cells (B) among pCAG-*Rb-TKO* cells (A,B) and pMAP2-*Rb-TKO* cells (C). (**D-F**) Immunofluorescent staining for GFP in the P2 telencephalon of control (D), *p107-single-Z* (E), and *Rb-TKO-Z* mice (F). The nuclei (cyan) were counterstained with DAPI and the images were merged. (**G**) Distribution of GFP-positive cells in control, *p107-single-Z* and *Rb-TKO-Z* mice. The cortical area was equally divided into five areas from the MZ to the VZ. **P*<0.05 [versus control (A-C) and versus control and *Rb-TKO* (G)]. Scale bar: 50 μm.

DNA repair induces EdU-incorporation, we added EdU and the topoisomerase inhibitor camptothecin, which causes DNA damage, for 16 hours before fixation. In the presence of 1 μM camptothecin, the ratio of the DNA damage marker phosphohistone H2AX (γ-H2AX)-positive cells was increased (supplementary material Fig. S3F) but that of EdU-positive cells was reduced (supplementary material Fig. S3G), suggesting that DNA repair did not lead to EdU incorporation in our experimental system. To determine whether these cells undergo G2/M-phase, we performed cell scoring for pH3. Interestingly, the ratio of pH3-positive cells was significantly increased in pCAG cells but not in pMAP2-*Rb-TKO* cells (Fig. 3F,G). Although the differentiating neurons of $Rb^{-/-}$ mice undergo massive apoptosis (Clarke et al., 1992; Jacks et al., 1992; Lee et al., 1992), no significant apoptosis was seen after Rb family inactivation, as previously reported in *Rb* conditional knockout mice (Ferguson et al., 2002; MacPherson et al., 2003) (supplementary material Fig. S3H,I). To determine whether the gene expression profiles of pCAG- and pMAP2-*Rb-TKO* cells reflect the differences in their cell cycle phases, we performed a genome-wide gene expression microarray analysis. A hierarchical clustering analysis revealed clear differences in the gene expression profiles between pCAG-*Rb-TKO* cells and pMAP2-*Rb-TKO* cells (supplementary material Fig. S4A). The Gene Ontology (GO) analysis of the upregulated genes of pCAG- and pMAP2-*Rb-TKO* cells revealed that genes involved in cell division, mitosis, chromosome segregation and DNA repair were significantly enriched only among the upregulated genes in the pCAG-*Rb-TKO* cells (Fig. 3H; supplementary material Table S2). By contrast, only genes involved in DNA replication were significantly enriched among the upregulated genes in both pCAG-*Rb-TKO* cells and pMAP2-*Rb-TKO* cells (Fig. 3H; supplementary material Table S2). No significant GO term was seen among the genes downregulated after Rb family inactivation (supplementary material Fig. S4B, Table S3), suggesting that the Rb family mainly act as a negative regulator of genes that are important for cell cycle progression during cortical development.

When the transfected cells were analyzed on P10 after *in utero* electroporation, the pCAG-*Rb-TKO* cells had expanded near the VZ (Fig. 4A,B). The Ki-67, EdU and pH3 staining analysis revealed that these expanded cells were highly proliferative and expressed Dcx (Fig. 4B-D), suggesting that *Rb-TKO* cortical progenitors continue to proliferate in the cerebral cortex. Although some of the expanding cells expressed Tbr2, these expanding cells did not express Nes, Gfap, Satb2, Ctip2 or Tbr1 (supplementary material Fig. S5). These results suggest that the expanding pCAG-*Rb-TKO* cells have the features of immature differentiating neurons.

Compensation by *p107* in the absence of *Rb* and *p130* in differentiating neurons

Compensation for Rb family members prevents tumor development in a context-specific manner (Ajioka and Dyer, 2008). Rb and p130 are expressed in retinal horizontal neurons, and *p107* compensates

for Rb family function in the regulation of the cell cycle in the absence of *Rb* and *p130*. However, *p107* is haploinsufficient for preventing proliferation and retinoblastoma development in retinal horizontal neurons (Ajioka et al., 2007). As basal progenitors and differentiating cortical neurons express Rb and p130 but not p107, we addressed whether one allele of *p107* can compensate for the function of Rb and p130. We used *Z/EG; $Rb^{Lox/Lox}$; $p107^{+/-}$; $p130^{Lox/Lox}$* (*p107-single-Z*) mice as well as *Z/EG; $Rb^{Lox/+}$; $p107^{-/-}$; $p130^{Lox/Lox}$* (*Rb-single-Z*) mice and *Z/EG; $Rb^{Lox/Lox}$; $p107^{-/-}$; $p130^{Lox/+}$* (*p130-single-Z*) mice. A cell scoring analysis demonstrated that one allele of *Rb* was sufficient for the cell cycle exit of progenitors and the prevention of cell cycle re-entry in differentiating neurons (Fig. 5A-C), similar to the results for retinal progenitors and neurons (Ajioka et al., 2007). Also, one allele of *p107* was sufficient to suppress cell cycle re-entry and to control the migration of differentiating cortical neurons (Fig. 5C-G). These results demonstrated that *p107* is haplosufficient in the absence of *Rb* and *p130* for Rb family functions in differentiating cortical excitatory neurons.

DSB repair pathway activation is essential for *Rb-TKO* differentiating neurons undergoing cell division

Interestingly, the GO analysis revealed that genes involved in DNA repair were significantly enriched only among the upregulated genes in the pCAG-*Rb-TKO* cells (Fig. 3H). To determine whether the DSB repair pathway is activated in pCAG-*Rb-TKO* differentiating neurons, GFP-positive cells were co-stained with the DSB marker γ-H2AX at P2. Many γ-H2AX-positive cells were detected in pCAG-*Rb-TKO* cells (Fig. 6A,C), but not in pMAP2-*Rb-TKO* cells (Fig. 6B), suggesting that the DSB repair pathway is activated only in pCAG-*Rb-TKO* cells. The Rb family is required for the trimethylation of H4K20 in mouse embryonic fibroblast (MEF), binding to histone methyltransferases Suv4-20h1 and Suv4-20h2 (Suv4-20h1/2) and causing the trimethylation of H4K20 from monomethylated H4K20 (Gonzalo et al., 2005). As the loss of *RB* or that of *Suv4-20h1/2* increased the monomethyl H4K20 (H4K20Me1) and the sensitivity of DNA damage stress (Bosco et al., 2004; Schotta et al., 2008), we examined the methylation status

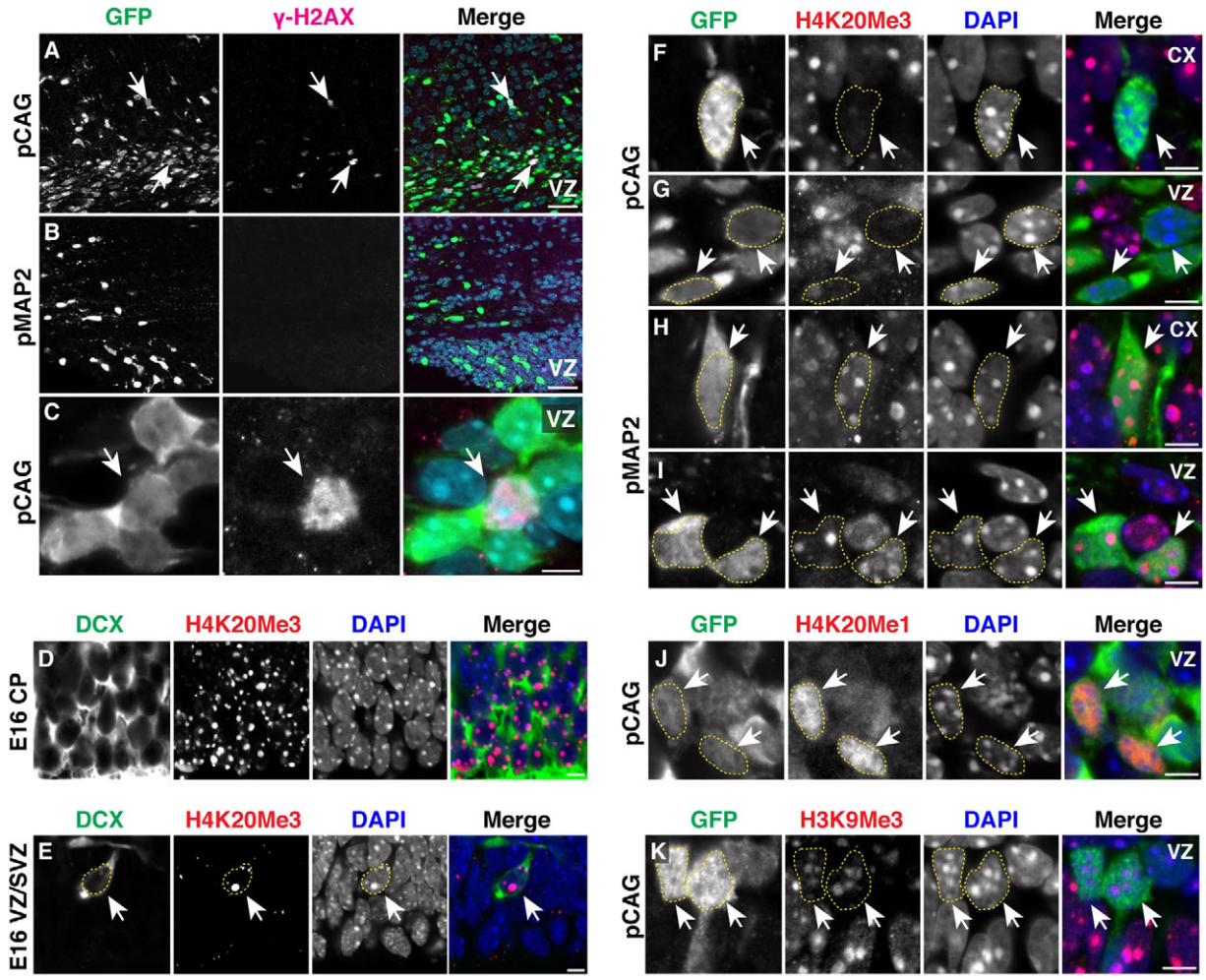

Fig. 6. DSB repair pathway activation without increase in H4K20Me3 in pCAG-*Rb-TKO* differentiating neurons. (**A-C**) Immunofluorescent staining for GFP (green) and γ-H2AX (magenta) in pCAG-Cre- (A,C) and pMAP2-Cre- (B) transfected P2 cerebral cortex from *Rb-TKO-Z* mice. The nuclei (cyan) were counterstained with DAPI and the images were merged. (**D**,**E**) Immunofluorescent staining for Dcx (green) and H4K20Me3 (red) in E16 CP (D) and VZ/SVZ (E). The DAPI (blue) staining images were merged. (**F-K**) Immunofluorescent staining for GFP (green) and H4K20Me3 (F-I), H4K20Me1 (J), or H3K9Me3 (K) (red) in pCAG-Cre- (F,G,J,K) and pMAP2-Cre- (H,I) transfected P2 cerebral cortex from *Rb-TKO-Z* mice at the VZ (G,I-K) and the CX (F,H). The DAPI (blue) staining images were merged. Scale bars: 50 μm in A,B; 5 μm in C-K.

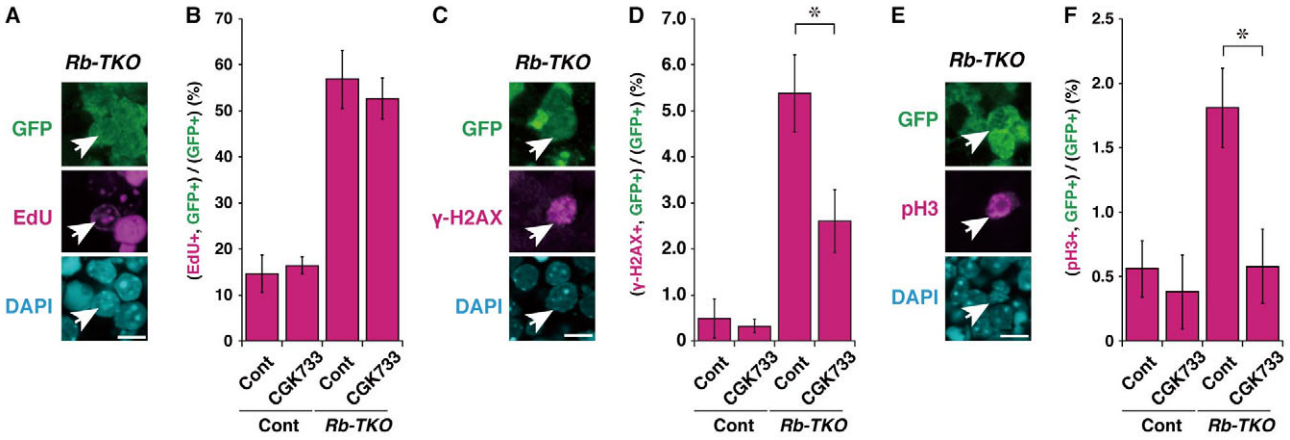

Fig. 7. DSB repair pathway is essential for the cell division of *Rb-TKO* differentiating neurons. (**A**,**C**,**E**) Immunofluorescent images for GFP (green), EdU (A), γ-H2AX (C), or pH3 (E) (magenta), and DAPI (cyan) in *Rb-TKO* cells. (**B**,**D**,**F**) Ratios of EdU (B), γ-H2AX (D), or pH3 (F) and GFP double-positive cells in the presence or absence of 10 μM CGK733 (ATM/ATR inhibitor). CGK733 and EdU were added to cortical explants for 16 hours before fixation. **P*<0.05. Scale bars: 10 μm.

of H4K20. During cerebral cortical development, trimethyl H4K20 (H4K20Me3) was detected in Dcx-positive cells at the pericentric heterochromatin in the CP and VZ/SVZ (Fig. 6D,E), suggesting that H4K20 is trimethylated just after neurogenesis. Interestingly, pCAG-*Rb-TKO* cells were not trimethylated at H4K20 (Fig. 6F,G), whereas pMAP2-*Rb-TKO* cells were trimethylated (Fig. 6H,I). In contrast to H4K20Me3, pCAG-*Rb-TKO* cells were monomethylated at H4K20 (Fig. 6J) and trimethylated at lysine 9 of histone H3 (H3K9) (Fig. 6K). To determine whether the DSB repair pathway is essential for the cell division of pCAG-*Rb-TKO* differentiating neurons, ataxia telangiectasia mutated (ATM)/ataxia telangiectasia and Rad3-related protein (ATR) (ATM/ATR) inhibitor (CGK733) was added to cortical explants. Although the ratio of EdU-positive cells was not changed in the presence of the ATM/ATR inhibitor (Fig. 7A,B), those of γ-H2AX- and pH3-positive cells were decreased (Fig. 7C-F). These results suggested that the DSB repair pathway is essential for the cell division of pCAG-*Rb-TKO* differentiating neurons.

DISCUSSION

After undergoing neurogenesis, differentiating cortical neurons become protected from DNA damage and cell division even in the absence of Rb family members. However, when cortical progenitors lose Rb family members, the daughter cells initiate differentiation without undergoing cell cycle exit and H4K20Me3 and proliferate.

Uncoupled proliferation and differentiation in the absence of Rb family members in cortical progenitors

During cortical development, even when cortical progenitors are forcibly suppressed from cell cycle exit by the overexpression of cyclins and cyclin-dependent kinases (CDKs) or the inhibition of CDK inhibitors (CKIs), the daughter cells maintain an undifferentiated state (Nguyen et al., 2006; Salomoni and Calegari, 2010). By contrast, when cortical progenitors lose Rb family members, the daughter cells initiate differentiation while maintaining an active cell cycle, suggesting the unique role of the Rb family in the coordination of cell cycle exit and the prevention of cortical progenitor differentiation. This idea is supported by the fact that human *RB*-deficient retinoblastoma expresses both progenitor and retinal neuron markers (McEvoy et al., 2011) and the fact that differentiated mouse *Chx10-Cre; $Rb^{Lox/Lox}$; $p107^{+/-}$; $p130^{-/-}$* horizontal interneurons in the retina proliferate while maintaining their differentiated features (Ajioka et al., 2007). In this study, we found that the expanding pCAG-*Rb-TKO* cells *in vivo* expressed the immature neuron marker Dcx, but not the glia marker or the neuronal layer markers. However, we do not exclude the possibility that these cells start to express other cortical cell markers at later stages. Further study is required to determine if the Rb family suppresses the gene expression that is specifically expressed in other cortical cells, as they do in the retina. Interestingly, once wild-type daughter cells start to differentiate, cell differentiation and proliferation begin to conflict with each other, even in the absence of Rb family members, in cortical excitatory neurons. The incompatibility of differentiation and proliferation, acquired epigenetically after neurogenesis, may be one of the mechanisms responsible for protecting long-life neurons from developing into tumors.

Overlapping roles of individual Rb family members in the development of cortical excitatory neurons

Since the discovery of *RB1* in patients with retinoblastoma (Friend et al., 1986) and the study of *Rb*-deficient mice (Clarke et al., 1992; Jacks et al., 1992; Lee et al., 1992), *Rb*, rather than *p107* and *p130*, has come to be regarded as the more vital gene for development and tumor suppression in the CNS. In fact, one allele of *Rb* is sufficient to suppress the cell cycle deregulation of cortical progenitors and differentiating neurons, as previously reported in the retina (Ajioka et al., 2007). Interestingly, the p107 and p130 proteins are complementally enriched with Rb protein during cortical development. p107 is expressed in apical progenitors, which produce both neurons and glia, while p130 is expressed in basal progenitors, which are more committed to produce neurons, and differentiating neurons. Although p107 expression is turned off during differentiation, one allele of *p107* was capable of compensating for Rb and p130 functions in differentiating neurons. Thus, careful genetic study that considers compensations and redundancies is required to examine the roles of Rb family members.

Rb is essential for the tangential migration of cortical interneurons, which are generated in the VZ of basal ganglia but not the cerebral cortex, in a cell-autonomous manner (Ferguson et al., 2005). *E2F3* and the suppression of the E2F3-target gene neogenin are essential for the tangential migration of cortical interneurons (Andrusiak et al., 2011; McClellan et al., 2007). *Rb* is also essential for the radial migration of cortical neurons in a non-cell-autonomous manner, possibly because of the loss of Cajal-Retzius cells, which are essential for radial migration because of the secretion of Reelin protein (Ferguson et al., 2005). However, the mechanism responsible for defective migration arising from the acute inactivation of all the Rb family members is different. First, one allele of *p107* rescued the migration defect. Second, the migration defect arising from the inactivating of all the Rb family members was cell autonomous. Third, the neogenin gene expression level was not changed in *Rb-TKO* cells in gene expression array data. Although we do not exclude the possibility that the migration defect of *Rb-TKO* was caused by altered differentiation and/or progenitor delamination, future study is thus required to reveal the mechanism by which Rb family members regulate radial migration.

DSB repair pathway activation for neuronal proliferation in the absence of Rb family

Rb is a transcriptional repressor of the E2F-target genes important for G1/S transition but also controls the G2/M transition by direct transcriptional regulations and epigenetic regulations (Sage and Straight, 2010). For example, the E2F-target gene *MAD2L1* encoding the mitotic checkpoint protein MAD2 is downregulated in *Rb*-deficient MEFs, which leads to genomic instability (Hernando et al., 2004). Also, Rb-dependent epigenetic modification protects against genomic instability by binding to the trimethylation enzyme of H4K20 Suv4-20h1/2 (Gonzalo et al., 2005). In the absence of all the Rb family members, the level of H4K20Me3 is decreased. Importantly, Suv4-20h1/2-deficient cells lose H4K20Me3, and their sensitivity to DNA damage increases (Schotta et al., 2008). Our study supports the important role of Rb-family-dependent epigenetic modifications for the G2/M arrest of differentiating cortical neurons *in vivo*. During the neurogenesis of cortical excitatory neurons, H4K20 was trimethylated. Once daughter cells initiate neuronal differentiation and are trimethylated at H4K20, the DSB repair pathway is not activated after the acute inactivation of Rb family members. However, differentiating neurons generated from *Rb-TKO* progenitors are not trimethylated at H4K20, and activate the DSB repair pathway. Thus, we propose that the Rb family plays an important role as direct transcriptional repressors of genes that are crucial for the G1/S transition in both progenitors and differentiating neurons and as an epigenetic protector of newly born neurons from DNA damage and the G2/M transition in progenitors during cerebral cortical development.

Acknowledgements
We thank Drs Li Foong Yoong and Takaki Miyata for discussions and Drs Michael Dyer, Anton Berns, Tyler Jacks, Julien Sage, Corrinne Lobe, Connie Cepko and Vijayasaradhi Setalurin for materials.

Funding
This work was supported by the Industrial Technological Research Grant Program in 2009 from the New Energy and Industrial Technology Development Organization (NEDO) of Japan, Grant-in-Aid for Scientific Research and the Strategic Research Program for Brain Sciences ('Understanding of molecular and environmental bases for brain health') of the Ministry of Education, Culture, Sports, Science and Technology (MEXT), the Takeda Science Foundation the Naito Foundation and the Canon Foundation.

Competing interests statement
The authors declare no competing financial interests.

Supplementary material
Supplementary material available online at
http://dev.biologists.org/lookup/suppl/doi:10.1242/dev.095653/-/DC1

References

Ajioka, I. and Dyer, M. A. (2008). A new model of tumor susceptibility following tumor suppressor gene inactivation. *Cell Cycle* **7**, 735-740.
Ajioka, I. and Nakajima, K. (2005). Birth-date-dependent segregation of the mouse cerebral cortical neurons in reaggregation cultures. *Eur. J. Neurosci.* **22**, 331-342.
Ajioka, I., Martins, R. A., Bayazitov, I. T., Donovan, S., Johnson, D. A., Frase, S., Cicero, S. A., Boyd, K., Zakharenko, S. S. and Dyer, M. A. (2007). Differentiated horizontal interneurons clonally expand to form metastatic retinoblastoma in mice. *Cell* **131**, 378-390.
al-Ubaidi, M. R., Hollyfield, J. G., Overbeek, P. A. and Baehr, W. (1992). Photoreceptor degeneration induced by the expression of simian virus 40 large tumor antigen in the retina of transgenic mice. *Proc. Natl. Acad. Sci. USA* **89**, 1194-1198.
Andrusiak, M. G., McClellan, K. A., Dugal-Tessier, D., Julian, L. M., Rodrigues, S. P., Park, D. S., Kennedy, T. E. and Slack, R. S. (2011). Rb/E2F regulates expression of neogenin during neuronal migration. *Mol. Cell. Biol.* **31**, 238-247.
Andrusiak, M. G., Vandenbosch, R., Park, D. S. and Slack, R. S. (2012). The retinoblastoma protein is essential for survival of postmitotic neurons. *J. Neurosci.* **32**, 14809-14814.
Becker, E. B. and Bonni, A. (2004). Cell cycle regulation of neuronal apoptosis in development and disease. *Prog. Neurobiol.* **72**, 1-25.
Bosco, E. E., Mayhew, C. N., Hennigan, R. F., Sage, J., Jacks, T. and Knudsen, E. S. (2004). RB signaling prevents replication-dependent DNA double-strand breaks following genotoxic insult. *Nucleic Acids Res.* **32**, 25-34.
Burkhart, D. L. and Sage, J. (2008). Cellular mechanisms of tumour suppression by the retinoblastoma gene. *Nat. Rev. Cancer* **8**, 671-682.
Chau, B. N. and Wang, J. Y. (2003). Coordinated regulation of life and death by RB. *Nat. Rev. Cancer* **3**, 130-138.
Chen, D., Livne-bar, I., Vanderluit, J. L., Slack, R. S., Agochiya, M. and Bremner, R. (2004). Cell-specific effects of RB or RB/p107 loss on retinal development implicate an intrinsically death-resistant cell-of-origin in retinoblastoma. *Cancer Cell* **5**, 539-551.
Clarke, A. R., Maandag, E. R., van Roon, M., van der Lugt, N. M., van der Valk, M., Hooper, M. L., Berns, A. and te Riele, H. (1992). Requirement for a functional Rb-1 gene in murine development. *Nature* **359**, 328-330.
Classon, M. and Harlow, E. (2002). The retinoblastoma tumour suppressor in development and cancer. *Nat. Rev. Cancer* **2**, 910-917.
Copani, A., Uberti, D., Sortino, M. A., Bruno, V., Nicoletti, F. and Memo, M. (2001). Activation of cell-cycle-associated proteins in neuronal death: a mandatory or dispensable path? *Trends Neurosci.* **24**, 25-31.
de Bruin, A., Wu, L., Saavedra, H. I., Wilson, P., Yang, Y., Rosol, T. J., Weinstein, M., Robinson, M. L. and Leone, G. (2003). Rb function in extraembryonic lineages suppresses apoptosis in the CNS of Rb-deficient mice. *Proc. Natl. Acad. Sci. USA* **100**, 6546-6551.
Dehay, C. and Kennedy, H. (2007). Cell-cycle control and cortical development. *Nat. Rev. Neurosci.* **8**, 438-450.
Donovan, S. L. and Dyer, M. A. (2007). Preparation and square wave electroporation of retinal explant cultures. *Nat. Protoc.* **1**, 2710-2718.
Donovan, S. L., Schweers, B., Martins, R., Johnson, D. and Dyer, M. A. (2006). Compensation by tumor suppressor genes during retinal development in mice and humans. *BMC Biol.* **4**, 14.
Feddersen, R. M., Ehlenfeldt, R., Yunis, W. S., Clark, H. B. and Orr, H. T. (1992). Disrupted cerebellar cortical development and progressive degeneration of Purkinje cells in SV40 T antigen transgenic mice. *Neuron* **9**, 955-966.
Feddersen, R. M., Clark, H. B., Yunis, W. S. and Orr, H. T. (1995). In vivo viability of postmitotic Purkinje neurons requires pRb family member function. *Mol. Cell. Neurosci.* **6**, 153-167.
Ferguson, K. L., Vanderluit, J. L., Hébert, J. M., McIntosh, W. C., Tibbo, E., MacLaurin, J. G., Park, D. S., Wallace, V. A., Vooijs, M., McConnell, S. K. et al. (2002). Telencephalon-specific Rb knockouts reveal enhanced neurogenesis, survival and abnormal cortical development. *EMBO J.* **21**, 3337-3346.
Ferguson, K. L., McClellan, K. A., Vanderluit, J. L., McIntosh, W. C., Schuurmans, C., Polleux, F. and Slack, R. S. (2005). A cell-autonomous requirement for the cell cycle regulatory protein, Rb, in neuronal migration. *EMBO J.* **24**, 4381-4391.
Friend, S. H., Bernards, R., Rogelj, S., Weinberg, R. A., Rapaport, J. M., Albert, D. M. and Dryja, T. P. (1986). A human DNA segment with properties of the gene that predisposes to retinoblastoma and osteosarcoma. *Nature* **323**, 643-646.

Gerdes, J., Lemke, H., Baisch, H., Wacker, H. H., Schwab, U. and Stein, H. (1984). Cell cycle analysis of a cell proliferation-associated human nuclear antigen defined by the monoclonal antibody Ki-67. *J. Immunol.* **133**, 1710-1715.
Gonzalo, S., García-Cao, M., Fraga, M. F., Schotta, G., Peters, A. H., Cotter, S. E., Eguía, R., Dean, D. C., Esteller, M., Jenuwein, T. et al. (2005). Role of the RB1 family in stabilizing histone methylation at constitutive heterochromatin. *Nat. Cell Biol.* **7**, 420-428.
Guillemot, F., Molnár, Z., Tarabykin, V. and Stoykova, A. (2006). Molecular mechanisms of cortical differentiation. *Eur. J. Neurosci.* **23**, 857-868.
Heintz, N. (1993). Cell death and the cell cycle: a relationship between transformation and neurodegeneration? *Trends Biochem. Sci.* **18**, 157-159.
Hernando, E., Nahlé, Z., Juan, G., Diaz-Rodriguez, E., Alaminos, M., Hemann, M., Michel, L., Mittal, V., Gerald, W., Benezra, R. et al. (2004). Rb inactivation promotes genomic instability by uncoupling cell cycle progression from mitotic control. *Nature* **430**, 797-802.
Herrup, K. and Yang, Y. (2007). Cell cycle regulation in the postmitotic neuron: oxymoron or new biology? *Nat. Rev. Neurosci.* **8**, 368-378.
Jacks, T., Fazeli, A., Schmitt, E. M., Bronson, R. T., Goodell, M. A. and Weinberg, R. A. (1992). Effects of an Rb mutation in the mouse. *Nature* **359**, 295-300.
Jiang, Z., Zacksenhaus, E., Gallie, B. L. and Phillips, R. A. (1997). The retinoblastoma gene family is differentially expressed during embryogenesis. *Oncogene* **14**, 1789-1797.
Kriegstein, A. and Alvarez-Buylla, A. (2009). The glial nature of embryonic and adult neural stem cells. *Annu. Rev. Neurosci.* **32**, 149-184.
Lee, E. Y., Chang, C. Y., Hu, N., Wang, Y. C., Lai, C. C., Herrup, K., Lee, W. H. and Bradley, A. (1992). Mice deficient for Rb are nonviable and show defects in neurogenesis and haematopoiesis. *Nature* **359**, 288-294.
Lee, E. Y., Hu, N., Yuan, S. S., Cox, L. A., Bradley, A., Lee, W. H. and Herrup, K. (1994). Dual roles of the retinoblastoma protein in cell cycle regulation and neuron differentiation. *Genes Dev.* **8**, 2008-2021.
MacPherson, D., Sage, J., Crowley, D., Trumpp, A., Bronson, R. T. and Jacks, T. (2003). Conditional mutation of Rb causes cell cycle defects without apoptosis in the central nervous system. *Mol. Cell. Biol.* **23**, 1044-1053.
MacPherson, D., Sage, J., Kim, T., Ho, D., McLaughlin, M. E. and Jacks, T. (2004). Cell type-specific effects of Rb deletion in the murine retina. *Genes Dev.* **18**, 1681-1694.
McClellan, K. A., Ruzhynsky, V. A., Douda, D. N., Vanderluit, J. L., Ferguson, K. L., Chen, D., Bremner, R., Park, D. S., Leone, G. and Slack, R. S. (2007). Unique requirement for Rb/E2F3 in neuronal migration: evidence for cell cycle-independent functions. *Mol. Cell. Biol.* **27**, 4825-4843.
McEvoy, J., Flores-Otero, J., Zhang, J., Nemeth, K., Brennan, R., Bradley, C., Krafcik, F., Rodriguez-Galindo, C., Wilson, M., Xiong, S. et al. (2011). Coexpression of normally incompatible developmental pathways in retinoblastoma genesis. *Cancer Cell* **20**, 260-275.
Nguyen, L., Besson, A., Roberts, J. M. and Guillemot, F. (2006). Coupling cell cycle exit, neuronal differentiation and migration in cortical neurogenesis. *Cell Cycle* **5**, 2314-2318.
Robanus-Maandag, E., Dekker, M., van der Valk, M., Carrozza, M. L., Jeanny, J. C., Dannenberg, J. H., Berns, A. and te Riele, H. (1998). p107 is a suppressor of retinoblastoma development in pRb-deficient mice. *Genes Dev.* **12**, 1599-1609.
Sage, J. and Straight, A. F. (2010). RB's original CIN? *Genes Dev.* **24**, 1329-1333.
Salomoni, P. and Calegari, F. (2010). Cell cycle control of mammalian neural stem cells: putting a speed limit on G1. *Trends Cell Biol.* **20**, 233-243.
Schotta, G., Sengupta, R., Kubicek, S., Malin, S., Kauer, M., Callén, E., Celeste, A., Pagani, M., Opravil, S., De La Rosa-Velazquez, I. A. et al. (2008). A chromatin-wide transition to H4K20 monomethylation impairs genome integrity and programmed DNA rearrangements in the mouse. *Genes Dev.* **22**, 2048-2061.
Tabata, H. and Nakajima, K. (2001). Efficient in utero gene transfer system to the developing mouse brain using electroporation: visualization of neuronal migration in the developing cortex. *Neuroscience* **103**, 865-872.
Tabata, H., Yoshinaga, S. and Nakajima, K. (2012). Cytoarchitecture of mouse and human subventricular zone in developing cerebral neocortex. *Exp. Brain Res.* **216**, 161-168.
Weinberg, R. A. (1995). The retinoblastoma protein and cell cycle control. *Cell* **81**, 323-330.
Zhang, J., Schweers, B. and Dyer, M. A. (2004). The first knockout mouse model of retinoblastoma. *Cell Cycle* **3**, 950-957.